



DØnote 4484-Conf, v1.3 - FINAL

## Search for Randall-Sundrum Gravitons in the Dielectron Channel with 200 pb<sup>-1</sup> of Data with the DØ Detector

The DØ Collaboration  
URL: <http://www-d0.fnal.gov>

(Dated: August 1, 2004)

We report preliminary results on a search for Kaluza-Klein gravitons in the Randall-Sundrum model with one “warped” extra dimension in the dielectron channel using  $\sim 200 \text{ pb}^{-1}$  of data collected in Run II of the Fermilab Tevatron. We find no indication of the effects of Randall-Sundrum gravitons and set limits on their mass for several values of the coupling to the SM fields. Graviton masses up to 660 GeV are ruled out at the 95% confidence level.

*Preliminary Results for Summer 2004 Conferences*

## I. INTRODUCTION

This analysis is a straightforward extension of the search for  $\text{TeV}^{-1}$  extra dimensions in the dielectron channel, described in detail in Ref. [1] and particularly the search for the  $Z'$  [2]. The data, background, efficiencies, and systematic errors are the same as in the former analyses. The extraction of limits on the Randall-Sundrum gravitons is based solely on the dielectron mass spectrum, shown in Fig. 1. Since the fraction of instrumental background is similar in the two topologies studied, where both electrons are in the central calorimeter cryostat (CC-CC) or one electron is in the central cryostat and one is in the end-cap cryostat (CC-EC), for the purpose of this search we combine spectra for these two topologies rather than performing a more involved, Bayesian fit for each topology and then combining the results by combining the likelihoods.

The present analysis is based on a counting experiment in a window around the assumed RS graviton mass, with the optimal width, which depends on the mass. The details of the method, all the systematics uncertainties, selection and cross section limits are the same as in the search for  $Z'$  [2], so they are repeated here only briefly.

## II. THE RANDALL-SUNDRUM MODEL OF EXTRA-DIMENSIONS

The phenomenological and experimental interest in high-dimensional physics has been considerably renewed recently, after it was realized that compactified extra-dimensions could yield observable effects at the current or foreseen experiments.

Models with extra space dimensions try to address the problem of the huge hierarchy between the Planck and the electroweak scales. The model proposed by Randall and Sundrum [3] (RS) considers the case of one “small” extra-dimension; the gravity is “localized” on a brane (Planck brane) apart from another brane where the SM fields are confined. The propagation of gravity in the extra-dimension is exponentially damped due to a fine-tuned space-time metric, resulting in the weakness of gravity when observed from the SM brane.

Since it propagates in the extra-dimension, the graviton observed in  $4d$  manifests itself as a “tower” of Kaluza-Klein (KK) modes, with the zero<sup>th</sup> mode corresponding to the massless graviton. In models of localized gravity the first graviton excitation  $G^{(1)}$  is expected to be heavy, with a mass around the TeV scale. Its coupling to all SM fields is solely determined by a dimensionless model parameter  $k/\bar{M}_{Pl}$ , in the range  $10^{-2} - 10^{-1}$ , and is expected to be sizeable.

Hence the spin 2 graviton  $G^{(1)}$  could be resonantly produced at the Tevatron via a  $q\bar{q}$  or a  $gg$  fusion. This model of extra-dimensions is investigated for the first time at the DØ experiment.

## III. SEARCH FOR RS GRAVITONS IN THE DIELECTRON CHANNEL

### A. Data Selection

The data used for this analysis was selected using all the available recent data from DØ Run II, i.e. data taken between April 2002 and November 2003. All the data have been reconstructed with the DØ reconstruction program (d0reco) version p14. These data correspond to the total integrated luminosity of  $\approx 200 \text{ pb}^{-1}$  and have been collected via a suit of single EM and diEM triggers, which run unscaled at all instantaneous luminosities. Given that the analysis is concerned only with high- $p_T$  EM objects, the trigger is  $99 \pm 1\%$  efficient for the signal.

We require two EM objects in the event, with the transverse energies above 25 GeV, which pass calorimeter energy isolation, EM energy fraction, and calorimeter shower shape cuts. At least one of the EM objects is required to have a matching track in the tracking detectors. Primary vertex in the event is defined via this track. We reject events that have more than two high- $p_T$  EM objects. The EM clusters are restricted to good fiducial volume of the DØ EM calorimeter:  $|\eta_d| < 1.1$  (CC) and  $1.5 < |\eta_d| < 2.4$  (EC), where  $\eta_d$  is pseudorapidity, as measured w.r.t. the geometrical center of the DØ detector.

For the detail of the preselection, see Ref. [4]. The overall efficiency of the event selection are as follows [1]:

$$\varepsilon_{\text{CC-CC}} = 0.74 \pm 0.02;$$

$$\varepsilon_{\text{CC-EC}} = 0.74 \pm 0.02; \tag{1}$$

$$\tag{2}$$

The analysis sample consists of 14,195 events, corresponding to 8,246 CC-CC and 5,949 CC-EC combinations. The event selection flow is detailed in Table I.

Cut	Number of events
Reconstructed Data	$\sim 700$ million events
NP diEM Stream	$\sim 2$ million events
Starting root-tuple sample after preselection	485K
$\geq 2$ EM objects w/ $E_T > 20$ GeV and $\chi^2$ cut	39,604
$E_T^{EM} > 25$ GeV, EMF cut, track match	15,602
At least one central EM object	14,195 = 8,246 CC-CC + 5,949 CC-EC

TABLE I: Event selection.

The integrated luminosity on this sample is known with 6.5% uncertainty (dominated by the uncertainty in the world average for the total inelastic cross section). In order to decrease the dependence on the luminosity measurement, we normalize all the cross sections to the NNLO  $Z$  production cross section, known well theoretically [5].

## B. Backgrounds

The QCD background is estimated via the method of Ref. [1]. The Drell-Yan background is simulated with the parton-level Monte Carlo generator of Ref. [4], augmented with a parametric simulation of the DØ detector. The simulation takes into account detector acceptance, efficiencies, and resolution, initial state radiation, and the effect of different parton distributions. We used leading order CTEQ4LO [6] distributions to estimate the nominal prediction. The parameters of the detector model are tuned using the  $Z(ee)$  data.

Since the parton-level generator involves only the  $2 \rightarrow 2$  hard-scattering process, we model next-to-leading order (NLO) effects by adding a transverse momentum to the diEM system, based on the measured transverse momentum spectrum of the  $Z(ee)$  events. Since the parton-level cross section is calculated at LO, we account for NLO effects in the SM background by scaling the cross sections by a constant  $K$ -factor of 1.3 [5].

The  $K$ -factor for  $Z/\gamma^*$  exchange tends to grow with mass [5]. Consequently, our assumption of a flat  $K$ -factor tends to underestimate the contribution from the SM (i.e., background) and thus is conservative in terms of sensitivity to the RS gravitons.

Since the direct diphoton production is at least an order of magnitude less than Drell-Yan production even at high masses, background from direct diphotons with photon conversions is negligible. All other physics backgrounds that result in dielectron final state are negligible.

## C. Systematics

We consider various sources of systematic uncertainties for signal and background, which are documented in Table II. Note that many sources of systematics are cancelled in the ratio of the  $Z$  and RS graviton cross sections; consequently when setting limits on RS gravitons, we use NNLO  $Z$  cross section in the  $e^+e^-$  channel of  $252 \pm 9$  pb [5] to determine the integrated luminosity in our sample, thus effectively normalizing graviton production cross section to that of the  $Z$ . The overall 9% signal cross section uncertainty includes  $E_T/\eta$  dependence of the efficiency of 7%, theoretical uncertainty on the NNLO  $Z$  cross section of 4%, and signal acceptance uncertainty of 5%. The central value of the integrated luminosity determined by this method corresponds to  $181 \text{ pb}^{-1}$ , in a good agreement with the  $196 \pm 13 \text{ pb}^{-1}$  from the DØ luminosity measurement.

Source of signal systematics	Uncertainty
$E_T$ and $\eta$ dependence of the efficiency	7%
Signal acceptance uncertainty	5%
$Z$ cross section uncertainty	4%
Total	9%
QCD background uncertainty	10%
DY background uncertainty	10%

TABLE II: Sources of systematic uncertainties used in this analysis.

The QCD background uncertainty stems from the uncertainty on normalization at low masses, which is slightly less than 10%; the DY background uncertainty mainly stem from the fact that we conservatively use a flat  $K$ -factor for DY, which results in 10% uncertainty due to the mass-dependence of the  $K$ -factor.

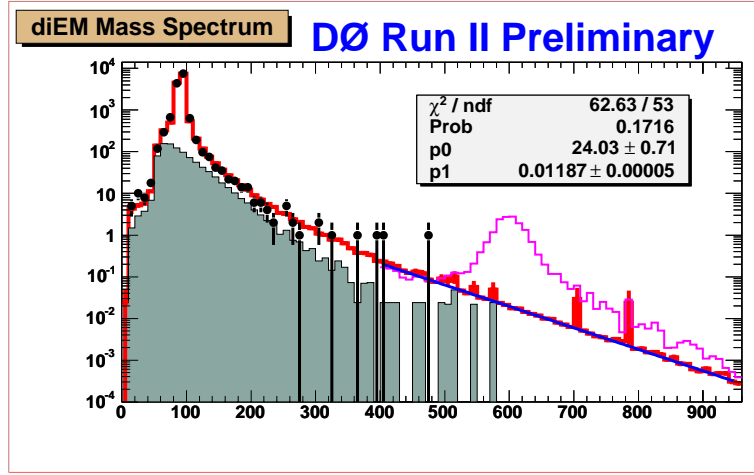


FIG. 1: Dielectron mass distribution. Points: data; shaded region: QCD background; open histogram: sum of the Drell-Yan and QCD background. Also shown: fit of the background at high masses to an exponent (blue solid line) and a shape of the  $G^{(1)}$  signal for the  $G^{(1)}$  mass of 600 GeV (magenta histogram). The fit parameter  $p1$  corresponds to the (negative) slope of the exponent, while  $p0$  reflects the normalization.

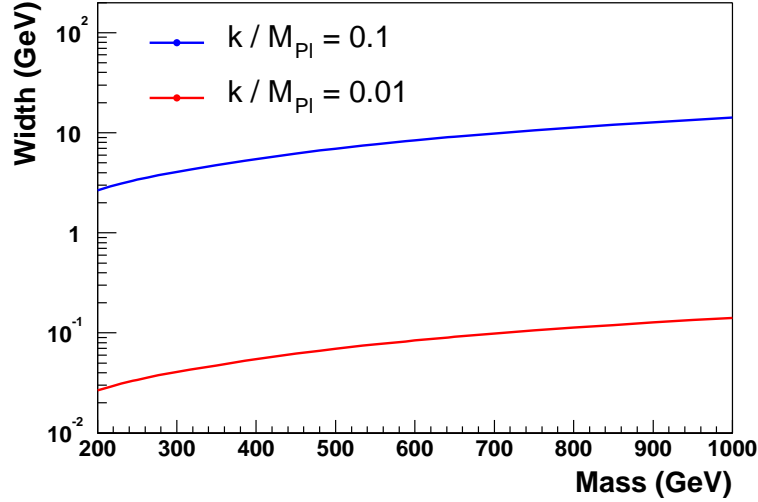


FIG. 2: Intrinsic width of the Randall-Sundrum gravitons as a function of their masses for two values of the coupling to the SM fields.

The intrinsic width of the RS gravitons  $G^{(1)}$  for the range of the parameters tested in this analysis (shown in Fig. 2), is small compared to the dielectron mass resolution of the DØ calorimeter. This is similar to the case of the search for  $Z'$ ; therefore we use the same counting window width as in the search for the  $Z'$  [2].

The results of the counting experiments in each mass window are summarized in Table III.

Since the data in each window are consistent with the expected background, we proceed with setting limits on the existence of the RS gravitons.

#### D. Acceptance Calculation

The acceptance and cross-section for the production of Randall-Sundrum gravitons for a coupling  $k/\bar{M}_{Pl} = 0.01$  was calculated using Pythia 6.202 [7] with CTEQ5L pdf's [8] and the DØ parametrized fast detector simulation for electron smearing based on the measured calorimeter resolution for electromagnetic objects.

The Pythia code for the production of Randall-Sundrum gravitons was modified following the relevant changes implemented in Pythia 6.224. No geometrical fiducial cuts are applied. Masses from 200–800 GeV were generated

TABLE III: Optimum window sizes and the results of the counting experiment in these windows.

RS Graviton Mass	Window	QCD bck.	DY bck.	Total bck.	Bck. Err	Data
200 GeV	190–210 GeV	13.0	15.6	28.6	2.9	26
300 GeV	280–320 GeV	1.6	4.3	5.9	0.59	3
400 GeV	380–420 GeV	0.14	1.05	1.19	0.12	2
500 GeV	450–550 GeV	0.16	0.70	0.86	0.09	1
600 GeV	540–660 GeV	0.05	0.26	0.31	0.03	0
700 GeV	620–780 GeV	0.05	0.11	0.16	0.02	0
800 GeV	700–900 GeV	0.05	0.05	0.09	0.01	0

TABLE IV: Leading order production cross-section and acceptances for  $G^{(1)} \rightarrow ee$  for a coupling  $k/\bar{M}_{Pl} = 0.01$  (from PYTHIA). The cross-sections scale as the square of  $k/\bar{M}_{Pl}$ . It was checked that setting  $k/\bar{M}_{Pl} = 0.1$  changes the acceptances by less than 2%. Only statistical uncertainties are shown.

$G^{(1)}$ Mass	$\sigma(RS) \times$ $B(RS \rightarrow ee)$	K-factor ( $K(M)$ )	Acceptance CC-CC	Acceptance CC-EC	Acceptance Total	Window cut efficiency
200 GeV	$1.011 \times 10^{-1}$ pb	1.30	$0.416 \pm 0.007$	$0.140 \pm 0.005$	$0.557 \pm 0.007$	0.878
300 GeV	$1.464 \times 10^{-2}$ pb	1.30	$0.484 \pm 0.007$	$0.137 \pm 0.005$	$0.621 \pm 0.007$	0.950
400 GeV	$3.773 \times 10^{-3}$ pb	1.30	$0.459 \pm 0.007$	$0.113 \pm 0.004$	$0.572 \pm 0.007$	0.879
500 GeV	$1.211 \times 10^{-3}$ pb	1.30	$0.541 \pm 0.007$	$0.099 \pm 0.004$	$0.640 \pm 0.007$	0.980
600 GeV	$4.454 \times 10^{-4}$ pb	1.30	$0.570 \pm 0.007$	$0.080 \pm 0.004$	$0.650 \pm 0.007$	0.977
700 GeV	$1.594 \times 10^{-4}$ pb	1.30	$0.572 \pm 0.007$	$0.064 \pm 0.003$	$0.636 \pm 0.007$	0.976
800 GeV	$5.634 \times 10^{-5}$ pb	1.30	$0.583 \pm 0.007$	$0.053 \pm 0.003$	$0.636 \pm 0.007$	0.978

with only the graviton production turned on at the generator level and its decays to electron pairs. Simulated events were accepted if two electrons had  $p_T > 25$  GeV/c at the generator level and were in the fiducial pseudorapidity range of  $|\eta| < 1.1$  (CC) or  $1.5 < |\eta| < 2.4$  (EC), with only CC-CC and CC-EC combinations being accepted. The invariant mass was calculated from the simulated electrons and the mass window cut of Table III was applied. Table IV shows the generated cross-section for  $G^{(1)} \rightarrow ee$  and the corresponding acceptances. The  $G^{(1)}$  events are slightly more central than the  $Z'$  ones due to the spin-2 nature of the graviton. The mass window cut is about 80% - 95% efficient at the higher masses (see tables) as events become much more central with higher graviton masses.

The statistical uncertainty is about 1% based on 10,000 event samples. A conservative overall 5% uncertainty is chosen to cover mass dependence of the pdf's and the acceptance dependence on the graviton couplings.

The LO PYTHIA cross section for RS production is multiplied by the flat  $K$ -factor of 1.3. (While no NLO calculations for RS graviton production exist yet, we assume the  $K$ -factor similar to that in the Drell-Yan or  $Z'$  production, as most of the NLO corrections come from the initial state radiation, which is similar in the case of DY and RS production. The  $K$ -factor and the cross section ratios are shown in Table IV.

#### E. Limits on the $G^{(1)}$ cross section and constraints on the Randall-Sundrum model

In order to set the limits on the  $G^{(1)} \rightarrow e^+e^-$  cross section, we use counting experiment in each mass window. We measure the effective integrated luminosity in our sample based on the central value of the NNLO  $Z(ee)$  cross section of  $252 \pm 9$  pb [5].

A standard Bayesian limit-setting procedure [9] with the signal and background systematics discussed above is applied. The results are listed in Table V and shown in Fig. 3 as a function of the  $G^{(1)}$  mass. Fig. 3 also shows the cross-sections predicted for various values of the coupling  $k/\bar{M}_{Pl}$ .

These limits can be translated into constraints on the parameters of the Randall-Sundrum model. The results are shown in Fig. 4 in the  $(k/\bar{M}_{Pl}, m_{G^{(1)}})$  plane. For a coupling  $k/\bar{M}_{Pl} = 0.1$  this analysis rules out Randall-Sundrum gravitons with masses below 660 GeV.

## IV. CONCLUSIONS

We performed a search for Randall-Sundrum gravitons decaying into the dielectron channel using  $\sim 200$  pb $^{-1}$  of data collected by the DØ Experiment at the Fermilab Tevatron in 2002-2003 (Run II). The data are in excellent agreement with Drell-Yan production and do not exhibit any evidence for new physics beyond the Standard Model, so

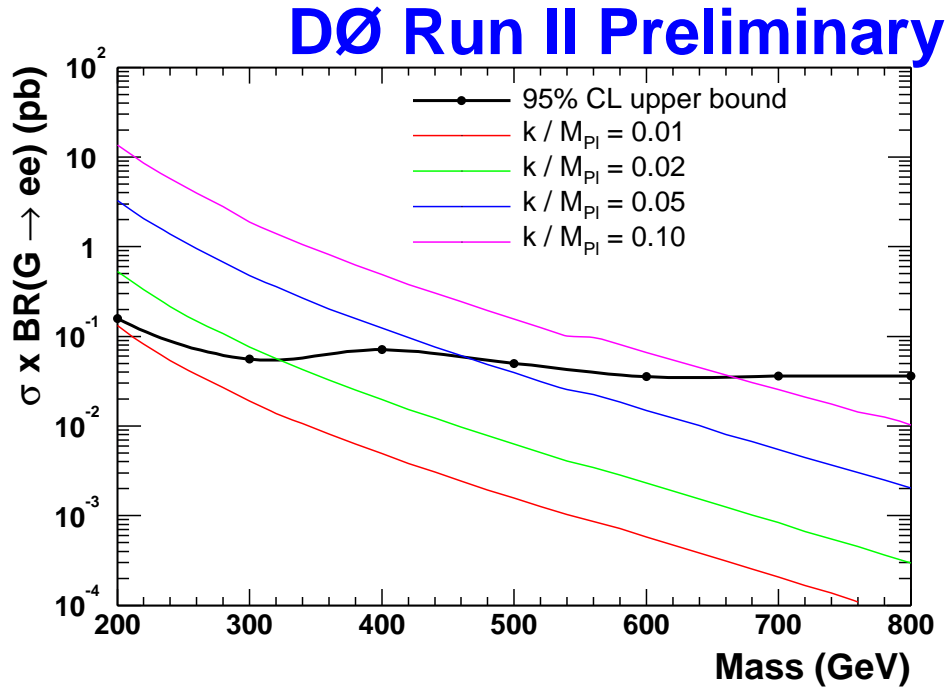


FIG. 3: Thick solid (black) curve: 95% CL upper bounds on the  $G^{(1)}$  production cross section times its branching fraction into  $ee$ . The other curves show the cross section times branching fraction predicted by the Randall-Sundrum model, for several values of the coupling  $k/\bar{M}_{Pl}$ .

TABLE V: Upper 95% CL limits on  $\sigma(G^{(1)} \rightarrow ee)$  as a function of the  $G^{(1)}$  mass.

$G^{(1)}$ Mass	$\sigma^{95}(G^{(1)} \rightarrow ee)$
200 GeV	158 fb
300 GeV	55.6 fb
400 GeV	71.0 fb
500 GeV	50.0 fb
600 GeV	35.4 fb
700 GeV	36.0 fb
800 GeV	36.0 fb

we use them to set limits on the existence of Randall-Sundrum gravitons. For a dimensionless coupling  $k/\bar{M}_{Pl} = 0.1$  Randall-Sundrum gravitons are ruled out at the 95% CL up to 660 GeV.

### Acknowledgments

We thank the staffs at Fermilab and collaborating institutions, and acknowledge support from the Department of Energy and National Science Foundation (USA), Commissariat à l'Energie Atomique and CNRS/Institut National de Physique Nucléaire et de Physique des Particules (France), Ministry of Education and Science, Agency for Atomic Energy and RF President Grants Program (Russia), CAPES, CNPq, FAPERJ, FAPESP and FUNDUNESP (Brazil), Departments of Atomic Energy and Science and Technology (India), Colciencias (Colombia), CONACyT (Mexico), KRF (Korea), CONICET and UBACyT (Argentina), The Foundation for Fundamental Research on Matter (The Netherlands), PPARC (United Kingdom), Ministry of Education (Czech Republic), Natural Sciences and Engineering Research Council and WestGrid Project (Canada), BMBF (Germany), A.P. Sloan Foundation, Civilian Research and Development Foundation, Research Corporation, Texas Advanced Research Program, and the Alexander von

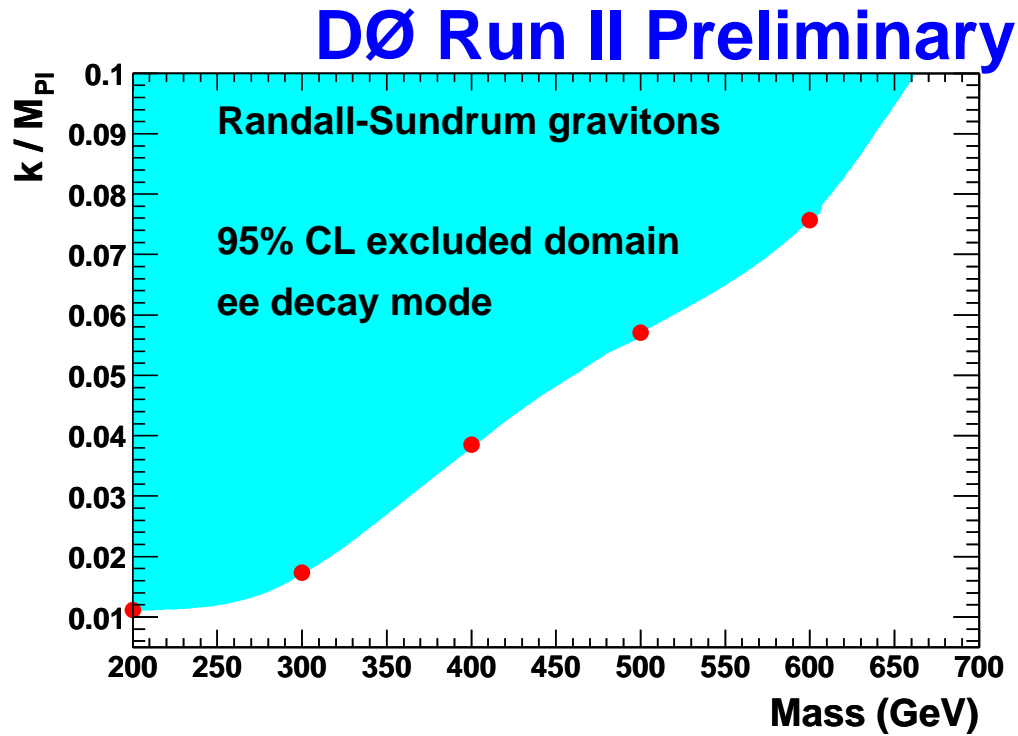


FIG. 4: Upper bounds at the 95% CL on the dimensionless coupling  $k/\bar{M}_{Pl}$  as a function of the mass of the first Kaluza-Klein graviton in the Randall-Sundrum model. Red dots show the mass points for which the cross section limits have been obtained in the analysis. The lower boundary of the exclusion region is a result of polynomial interpolation between these points. Note that for masses above 500 GeV, signal windows overlap, thus ensuring no gaps in the mass-spectrum coverage.

Humboldt Foundation.

- 
- [1] DØ Collaboration, DØ Note 4349-Conf (2004),  
<http://www-d0.fnal.gov/Run2Physics/WWW/results/NP/NP02.pdf>.
  - [2] DØ Collaboration, DØ Note 4375-Conf (2004),  
<http://www-d0.fnal.gov/Run2Physics/WWW/results/NP/NP03.pdf>
  - [3] L. Randall and R. Sundrum, Phys. Rev. Lett. **83**, 3370 (1999).
  - [4] DØ Collaboration, DØ Note 4336-Conf,  
<http://www-d0.fnal.gov/Run2Physics/WWW/results/NP/NP01.pdf>.
  - [5] R. Hamberg, W.L. Van Neerven, and T. Matsura, Nucl. Phys. B**359**, 343 (1991).
  - [6] H.L. Lai *et al.* (CTEQ Collaboration), Phys. Rev. **D51**, 4763 (1995).
  - [7] T. Sjostrand, P. Eden, C. Friberg, L. Lonnblad, G. Miu, S. Mrenna, and E. Norrbin, Comp. Phys. Comm. **135**, 238 (2001).
  - [8] H.L. Lai *et al.* (CTEQ Collaboration), Eur. Phys. J. C **12**, 375 (2000).
  - [9] I. Bertram *et al.* preprint Fermilab-TM-2104 (2000).